JCTC Journal of Chemical Theory and Computation

A QTAIM and Electron Delocalization Computational Study of *tert*-Butylmethylene, Trimethylsilylmethylene, and Trimethylgermylmethylene. A New Method for Unambiguously Characterizing the Bonding between Pairs of Atoms in Reaction Intermediates

Daniel A. Poulsen and Nick H. Werstiuk*

Department of Chemistry, McMaster University, Hamilton, ON, Canada L8S 4M1

Received July 1, 2005

Abstract: While studies on the experimental photolytic and thermolytic extrusion of nitrogen from *tert*-butyldiazomethane and *tert*-butyldiazirine and the decomposition of other precursors have shown a mixture of C−H and C−C insertion products depending on conditions, the analogous trimethylsilyldiazomethane undergoes solely Si−C insertion. Description of the singlet *tert*-butylmethylene intermediates potentially involved in the C−H and C−C insertion reactions and were addressed through computational means by Armstrong et al. (*J. Am. Chem. Soc.* **1995**, *117*, 3685−3689). In addition to re-examining singlet *tert*-butylmethylene at a higher level of theory [CCSD/6-311+G(d,p)], we have studied the silicon and germanium analogues trimethylsilylmethylene and trimethylgermylmethylene. A computational atoms-in-molecules and atomic-basin-delocalization-indices analysis established that the singlet carbenes, while exhibiting varying degrees of delocalization, are not bridged species based on the fact that none possess a pentacoordinate methyl group. In addition, from the results, we are able to make a prediction of solely a Ge−C insertion product for the extrusion of nitrogen from trimethylgermyldiazomethane. Most importantly, we demonstrated that a combination of quantum theory of atoms in molecules (QTAIM) molecular graphs, the evaluation of delocalization indices, and a visualization of the closeness of atomic basins—a QTAIM-DI-VISAB analysis—should be considered as the method of choice for unambiguously characterizing the bonding between pairs of atoms not only of carbenes but of other reaction intermediates such as carbocations, carbanions, and radicals.

Introduction

The photolytic and thermolytic extrusion of nitrogen from *tert*-butyldiazomethane and *tert*-butyldiazirine has been experimentally shown to proceed to the C−H insertion product, 1,1-dimethylcyclopropane, and the C−C insertion product, 2-methyl-2-butene, in ratios dependent on the conditions and method of decomposition.[1] While the involvement of excited states of diazirines and diazo compounds can complicate the situation in the photolytic decompositions, it is generally agreed that singlet carbenes, as the first-formed intermediates in thermal processes, can yield insertion and rearrangement products.[2] The complexities of the formation and reactions of *tert*-butylmethylene have been summarized in a paper by Glick and co-workers.[3] The trimethylsilyldiazomethane analogue of *tert*-butyldiazomethane has been reported to undergo similar decomposition, however, only producing the Si−C insertion product trimethylsilene.[4,5] To date, there have been no known experimental reports on the results of decomposition of the Ge analogue.

Various conformations of the carbene *tert*-butylmethylene [:CHC$(CH_3)_3$] and their reactions have been previously

* Corresponding author phone: (905) 525-9140 ext. 23482; e-mail: werstiuk@mcmaster.ca.

10.1021/ct0501654 CCC: $33.50
Published on Web 12/14/2005

Table 1. Energies of Intermediate Carbenes

carbene	Figure	gradient level of theory	CCSD[a]	MP2[b]	ZPE[c]	relative CCSD[d]
syn-tert-butylmethylene	1	MP2/6-31G(d)		−195.661 330	90.180	
syn-tert-butylmethylene	2	CCSD/6-311+G(d,p)	−195.884 009	−195.817 432	88.428	0.000 00
anti-tert-butylmethylene	3	CCSD/6-311+G(d,p)	−195.883 886	−195.814 133	88.310	0.077 18
anti-trimethylsilylmethylene[e]		MP2/6-311+G(d,p)		−446.840 472	83.061	
anti-trimethylsilylmethylene	4	CCSD/6-311+G(d,p)	−446.918 554	−446.840 273	82.927	
anti-trimethylgermylmethylene[e]		MP2/6-311+G(d,p)		−2233.205 448	82.495	
anti-trimethylgermylmethylene	5	CCSD/6-311+G(d,p)	−2233.282 625	−2233.205 302	82.374	

[a] CCSD energy/hartrees. [b] MP2 energy/hartrees. [c] Zero-point energy at 298 K and 1 atm/kcal mol^{-1}. [d] Relative CCSD energy/kcal mol^{-1}. [e] Figures available in the Supporting Information.

investigated through computational methods.[6] However, conclusions about bonding interactions in these intermediates have, until now, been based on the appearance of molecular geometry and not molecular structure. Like other reaction intermediates such as carbocations, carbanions, and radicals, carbenes are prime candidates for analysis by the quantum theory of atoms in molecules (QTAIM)[7] and delocalization and localization indices (DIs and LIs). QTAIM provides a universal indicator of bonding between atoms[8] in the form of a shared interatomic surface with the number of bond paths terminating at the nucleus defining the coordination at an atom and thereby providing an unambiguous definition of bridging. Delocalization between pairs of atomic basins not exhibiting a bond path may also be investigated through the calculation of DIs.[9,10] In our view, the combination of QTAIM molecular graphs, the evaluation of DIs, and a visualization of the atomic basin proximity at isosurface density values in the range of 0.001−0.005 au—the QTAIM-DI-VISAB analysis—should be considered as the method of choice for unambiguously characterizing the bonding between pairs of atoms in transient intermediates and stable molecules.[11]

This computational study presents data that lead to a refinement of the conclusions regarding bonding reached in the previous treatment of *tert*-butylmethylene carbene and presents computational results on the Si and Ge analogues trimethylsilylmethylene [:CHSi(CH_3)$_3$] and trimethylgermylmethylene [:CHGe(CH_3)$_3$]; we report the results of a QTAIM-DI-VISAB analysis of the bonding in these intermediates.

Computational Methods

Singlet carbene geometries were optimized at MP2/6-31G(d), MP2/6-311+G(d,p), MP2/cc-pVTZ, and CCSD/6-311+G(d,p) levels with Gaussian 03.[12] Frequency calculations were made on the resulting stationary points to confirm them as energy minima. Coupled cluster with single and double excitation (CCSD) minima were confirmed with Moeller−Plesset second-order (MP2) frequency calculations using the same basis set. QTAIM analyses of the wave functions to investigate the topology of the electron densities of the optimized intermediates were carried out with AIM2000,[13] and AIMALL97[14] was used to integrate the atomic basins and obtain the atomic overlap matrices required for DI calculations. The program LI-DICALC[9] was used to obtain the DIs.

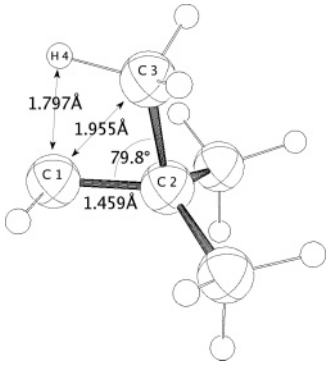

Figure 1. MP2/6-31G(d) *tert*-butylmethylene molecular geometry.

Results and Discussion

We have found that the MP2/6-31G(d) geometry, Figure 1, presented by Armstrong et al.[6] does not exhibit a bond critical point between the carbenic carbon (C1) and the closest methyl carbon (C3) at 1.955 Å, indicating that this minimum-energy geometrical structure should not be considered a bridged species; C3 does not have five bond paths terminating at the nucleus! Nevertheless, the DI between carbenic carbon C1 and C3 (0.278) is higher than the indices between it and both other methyl carbon atoms (0.05), confirming significant electron delocalization afforded by this unsymmetrical geometry. The hydrogen atom H4 also shows a higher DI with C1 than those found on the other two methyl groups; however, no bond critical point exists between them. This intermediate illustrates delocalization without hypervalent bridging, which can be unambiguously defined on the basis of the number of bond paths terminating at the nucleus. Interestingly, we found that this geometry was not an energy minimum using the larger basis sets 6-311+G(d,p) and cc-pVTZ, raising questions as to its validity at the MP2 level.

Calculations at the CCSD/6-311+G(d,p) level yielded two energy-minimum geometries, Figures 2 and 3. These differ in the dihedral angle between the carbenic carbon and the methyl proton. In one, H4 is syn to C1, and in the other, H4 is anti to C1. As seen in the molecular graph, Figures 4 and 5, respectively, no bond critical point or bond path was found between C1 and C3 in either of these geometries and no bond path is seen between H4 and C1 of the syn species. The syn conformation appears similar to the one previously reported at MP2/6-31G(d); however, the C1−C2−C3 angle is larger at 85.2°, implying even less delocalization at this CCSD level. This was confirmed by the atomic basin delocalization analysis, which produced a DI of 0.193

Table 2. Atomic Basin Delocalization Indices

carbene	Figure	level of theory	delocalization index C1−C3	C1−H4	X2−C1[a]	X2−C3[a]
syn-tert-butylmethylene	1	MP2/6-31G(d)	0.278	0.128	0.966	0.737
syn-tert-butylmethylene	2	CCSD/6-311+G(d,p)	0.193	0.103	0.939	0.748
anti-tert-butylmethylene	3	CCSD/6-311+G(d,p)	0.119		0.938	0.763
anti-trimethylsilylmethylene[b]		MP2/6-311+G(d,p)	0.188		0.453	0.399
anti-trimethylsilylmethylene	4	CCSD/6-311+G(d,p)	0.149		0.438	0.400
anti-trimethylgermylmethylene[b]		MP2/6-311+G(d,p)	0.101		0.726	0.646
anti-trimethylgermylmethylene	5	CCSD/6-311+G(d,p)	0.078		0.699	0.643

[a] Where X is C, Si, or Ge. [b] Figures available in the Supporting Information.

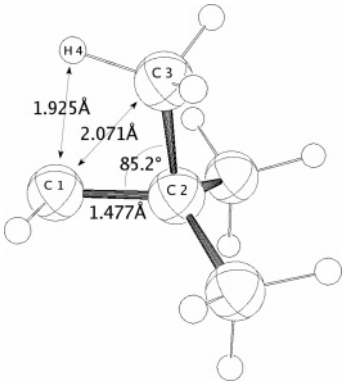

Figure 2. CCSD/6-311+G(d,p) *syn-tert*-butylmethylene molecular geometry.

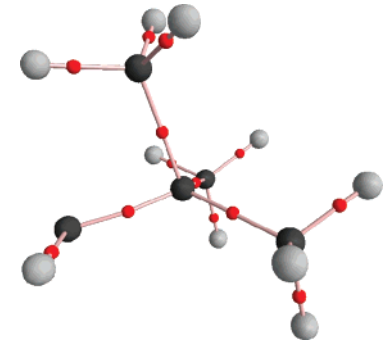

Figure 4. CCSD/6-311+G(d,p) *syn-tert*-butylmethylene molecular graph. The (3,−1) bond critical points are shown as red spheres.

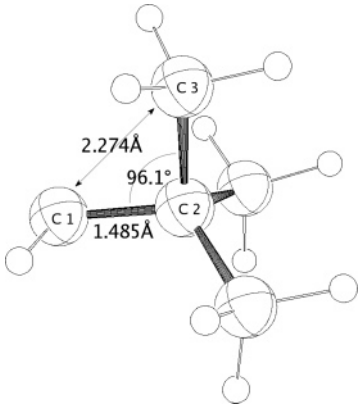

Figure 3. CCSD/6-311+G(d,p) *anti-tert*-butylmethylene molecular geometry.

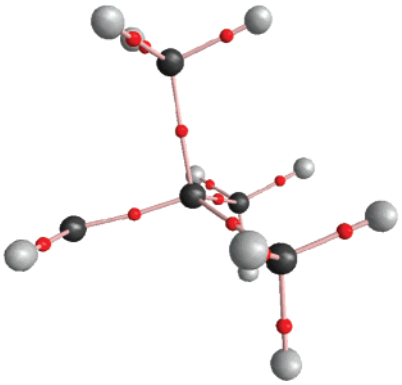

Figure 5. CCSD/6-311+G(d,p) *anti-tert*-butylmethylene molecular graph.

between the C1 and C3 basins compared to 0.278 for the geometry at MP2/6-31G(d). The DI between H4 and C1 of the syn conformer is 0.103 at the CCSD/6-311+G(d,p) level, somewhat less than the value of 0.193 found at MP2/6-31G(d). The DI between H4 and C1 also indicates that significant delocalization, similar to that found between C1 and C3, is not necessarily accompanied by bridging as defined by QTAIM. These carbenes clearly exhibit diffuse electron density which is delocalized into all proximate basins without requiring bridging to each of them.

The difference in energy between the syn and anti species is negligible, with syn more stable than anti by 0.077 kcal/mol. Although both geometries are of essentially equal energy, the delocalization indices between C1 and C3 are quite different at 0.193 and 0.119 for Figures 2 and 3, respectively. This difference is accompanied by minor changes in the delocalization between the central C2 and both the carbenic carbon C1 and methyl group carbon C3. We believe that there are two factors affecting the stability of these intermediates. Delocalization that is stabilizing is the first factor, and it favors both of these unsymmetrical geometries over one with C_s symmetry. The second is destabilizing strain introduced by decreasing the C1−C2−C3 angle. The reason these two geometries are of nearly equal energy is that stabilization achieved in the syn conformation by increased delocalization between C1 and C3 as well as C1 and H4 (DI = 0.103) is countered by the destabilizing effect of decreasing this angle relative to the anti conformation. This analysis indicates that delocalization plays a role in stabilizing these carbenes by favoring the unsymmetrical conformations, but it does not result in the formation of bond paths between the carbenic carbon C1 and C3. These carbenes are far from being bridged species in the QTAIM sense.

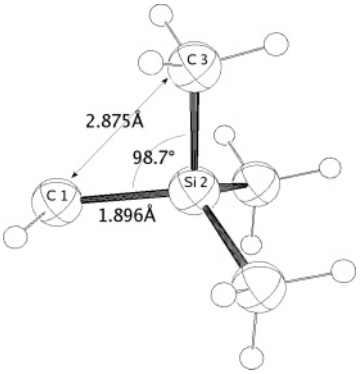

Figure 6. CCSD/6-311+G(d,p) trimethylsilylmethylene molecular geometry.

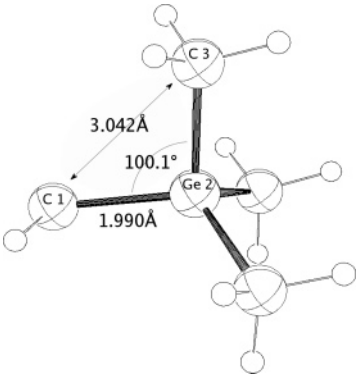

Figure 7. CCSD/6-311+G(d,p) trimethylgermylmethylene molecular geometry.

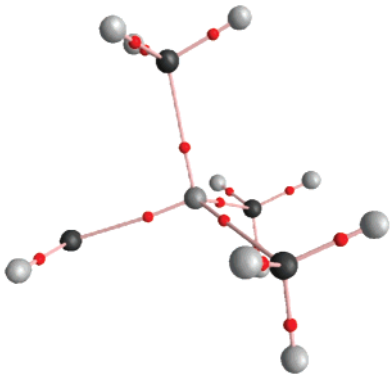

Figure 8. CCSD/6-311+G(d,p) trimethylsilylmethylene molecular graph.

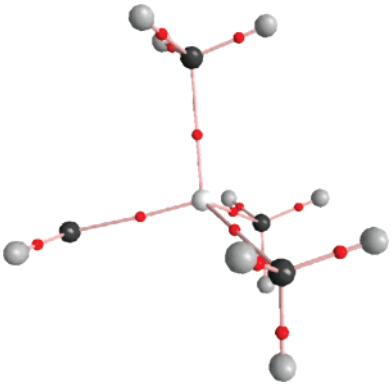

Figure 9. CCSD/6-311+G(d,p) trimethylgermylmethylene molecular graph.

The fact that trimethylsilyldiazomethane does not show C−H insertion upon pyrolysis can be attributed to increased ring strain in the resulting trimethylcylclopropasilane. This is due to a larger Si−C bond distance, making the C−Si−C angle much smaller, at the B3PW91/6-311+G(d,p) level, a C−Si bond length of 1.854 Å and a C1−Si2−C3 angle of 49.8°. The likelihood of the three-member ring is even worse for the germanium analogue, where the carbon−germanium bond distance is even greater, at the B3PW91/6-311+G(d,p) level, a C−Ge bond length of 1.947 Å and C1−Ge2−C3 angle of 46.7°.

We have found similar energy-minimum geometries for the carbenes trimethylsilylmethylene [:CHSi$(CH_3)_3$] and trimethylgermylmethylene [:CHGe$(CH_3)_3$], as seen in Figures 6 and 7, respectively. QTAIM analysis yields no critical point between C1 and C3 in either of these intermediates, as seen in the molecular graphs in Figures 8 and 9. These carbenes exist with H4 of the C3 methyl group anti to the carbenic carbon C1, while the corresponding syn geometry found for *tert*-butylmethylene is no longer an energy minimum for either analogue. The rationale for this, once again, being the effect of increasing the bond length to the central atom. As a result of this distance increase, the delocalization interaction between C1−C3 and C1−H4 is sacrificed owing to the destabilization of the required decrease in the C1−X2−C3 angle. This is consistent with the experimental observations of solely a Si−C insertion product for the decomposition of *tert*-butyldiazomethane.[4,5] The anti geometry is unlikely to undergo C−H insertion with the hydrogen atom out of the plane defined by C1−Si2−C3. Considering the similar geometry of trimethylgermylmethylene, we predict that the extrusion of nitrogen from trimethylgermyldiazomethane will occur in a similar route through Ge−C insertion.

In addition to quantitative results from the QTAIM analysis and atomic basin DIs, we have also plotted several basin surfaces. These plots clearly show the qualitative characteristics of the atomic basin DIs of interest. It is known that an isosurface density value of 0.001 au accounts for 99% of the electronic charge for carbon and can be used to define the van der Waals shape as discussed by Bader.[7] We present plots at an isosurface density value of 0.005 au because the surface is significantly smoother as per limitations of the rendering in AIM2000.[13] In any case, these basins account for even less electronic charge yet still provide a means to visually inspect the relative distances between basins and, therefore, confirm the DI results. Figures 10 and 11 highlight the difference in delocalization for the CCSD/6-311+G(d,p) *syn-tert*-butylmethylene intermediate between the C3 methyl group and the other two. In Figure 10, the C3 basin is in very close proximity with the C1 carbenic basin at an isosurface density value of 0.005 au with a DI of 0.193, while in Figure 11, the C5 basin is significantly separated from C1 with a DI of 0.050. This is consistent with the DI results discussed previously and gives visual confirmation of the basin delocalization for this unsymmetrical intermediate. It is also interesting to note the significant contribution of delocalization between the C1 and H4 basins for the syn orientation. The shape of the H4 basin, shown in Figure 12,

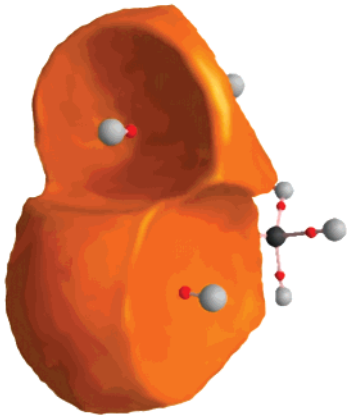

Figure 10. CCSD/6-311+G(d,p) *syn-tert*-butylmethylene molecular graph with atomic basin C1 and C3 density isosurface 0.005.

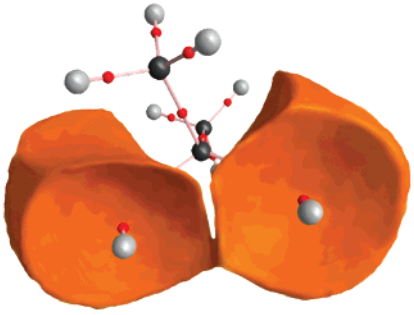

Figure 11. CCSD/6-311+G(d,p) *syn-tert*-butylmethylene molecular graph with atomic basin C1 and C5 density isosurface 0.005.

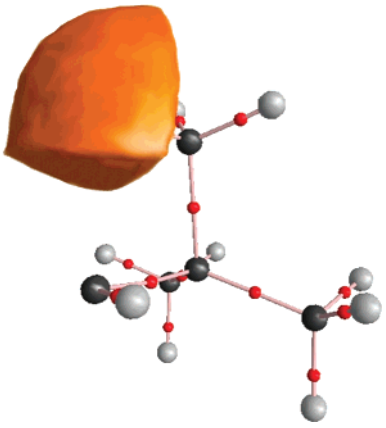

Figure 12. CCSD/6-311+G(d,p) *syn-tert*-butylmethylene molecular graph with atomic basin H4 density isosurface 0.005.

indicates clear deformation caused by the very close proximity of the C1 basin and vice versa, consistent with a DI of 0.103. Figure 10 also clearly illustrates the nearness of the H4 and C1 basins through apparent impingement on each other: Figure 11 clearly shows how the C1 basin is perturbed as a result of the closeness of H4 relative to the C5 basin.

Similar plots of the C1 and C3 basins are presented here for the *anti-tert*-butylmethylene, *anti*-trimethylsilylmethylene, and *anti*-trimethylgermylmethylene intermediates in Figures 13, 14, and 15, respectively. This series highlights the C1 and C3 delocalization difference across the three anti

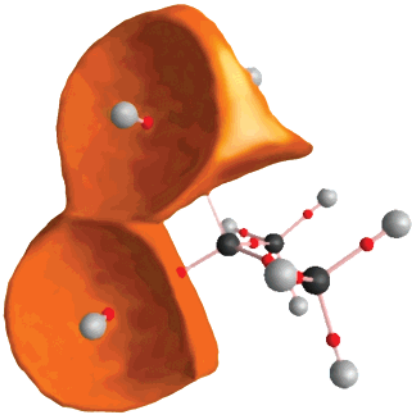

Figure 13. CCSD/6-311+G(d,p) *anti-tert*-butylmethylene molecular graph with atomic basin C1 and C3 density isosurface 0.005.

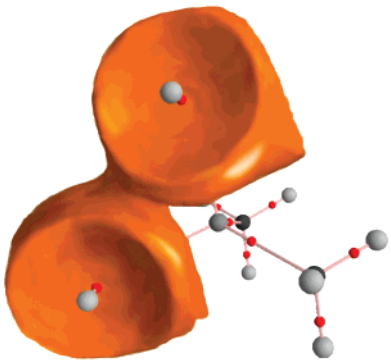

Figure 14. CCSD/6-311+G(d,p) trimethylsilylmethylene molecular graph with atomic basin C1 and C3 density isosurface 0.005.

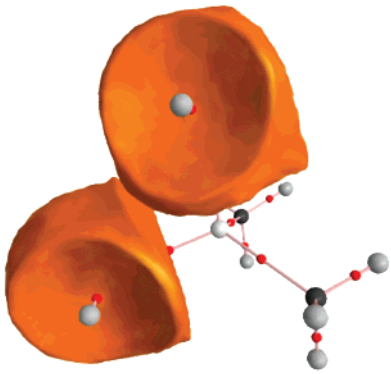

Figure 15. CCSD/6-311+G(d,p) trimethylgermylmethylene molecular graph with atomic basin C1 and C3 density isosurface 0.005.

intermediates which differ in the central atom. At isosurface 0.005, the basins for *anti-tert*-butylmethylene and *anti*-trimethylsilylmethylene are very close to each other, with the DIs being 0.119 and 0.149, respectively, while this is not the case for trimethylgermylmethylene (see Figure 15) with a DI of 0.078.

Conclusions

Using QTAIM, we have shown that free singlet *tert*-butylmethylene does not possess a pentacoordiante methyl

group and, therefore, is not bridged. Two novel geometries have been presented at the CCSD/6-311+G(d,p) level which show a syn and anti conformation with nearly the same energy, $\Delta = 0.077\ 18$ kcal/mol. Delocalization does play a role in stabilizing these carbenes by favoring the unsymmetrical conformations, but they are far from being any sort of bridged species.

Similar intermediate geometries were found for the silicon and germanium analogues, trimethylsilylmethylene and trimethylgermylmethylene; however, the syn conformation was not an energy minimum. This can be attributed to an increase in the Si−C and Ge−C bond lengths. These unsymmetrical carbenes also showed no sign of being bridged species; they do not exhibit pentacoordinate methyl groups. They are stabilized by minor delocalization between a methyl carbon and the carbenic carbon. Our analysis is consistent with experimental findings to date[1,3−5] and is able to predict that the extrusion of nitrogen from trimethylgermyldiazomethane will result in solely the Ge−C insertion product. Most importantly, this paper clearly demonstrates that the combination of QTAIM molecular graphs, the evaluation of DIs, and a visualization of the closeness or atomic basins at isosurface density values in the range of 0.001−0.005 au—a QTAIM-DI-VISAB analysis—should be considered as the method of choice for unambiguously characterizing the bonding between pairs of atoms not only of carbenes but of other reaction intermediates such as carbocations, carbanions, and radicals.

Acknowledgment. We thank the Natural Sciences and Engineering Research Council of Canada for the support making this study possible. We also thank the Shared Hierarchical Academic Research Computing Network (SHARCNET) of Ontario for CPU time necessary for several geometry optimizations.

Supporting Information Available: Figures for *anti*-trimethylsilylmethylene and *anti*-trimethylgermylmethylene at the MP2/6-311+G(d,p) level. This material is available free of charge via the Internet at http://pubs.acs.org.

References

(1) Chang, K. T.; Shechter, H. *J. Am. Chem. Soc.* **1979**, *101*, 5082.

(2) Nickon, A. *Acc. Chem. Res.* **1993**, *26*, 84.

(3) Glick, H. C.; Likhotvorik, I. R.; Jones, M., Jr. *Tetrahedron Lett.* **1995**, *36*, 5715.

(4) Chedekel, M. R.; Skoglund, M.; Kreeger, R. L.; Shechter, H. *J. Am. Chem. Soc.* **1976**, *98*, 7848.

(5) Kreeger, R. L.; Shechter, H. *Tetrahedron Lett.* **1975**, *25*, 2061.

(6) Armstong, B. M.; McKee, M. L.; Shevlin, P. B. *J. Am. Chem. Soc.* **1995**, *117*, 3685.

(7) Bader, R. F. W. *Atoms in Molecules − A Quantum Theory*; Oxford University Press: New York, 1990.

(8) Bader, R. F. W. *J. Phys. Chem. A* **1998**, *102*, 7314.

(9) Wang, Y.; Matta, C.; Werstiuk, N. H. *J. Comput. Chem.* **2003**, *24*, 1720.

(10) Wang, Y.; Werstiuk, N. H. *J. Comput. Chem.* **2003**, *24*, 379.

(11) Bajorek, T.; Werstiuk, N. H. *Can. J. Chem.* **2005**, *83*, 1352.

(12) Frisch, M. J.; Trucks, G. W.; Schlegel, H. B.; Scuseria, G. E.; Robb, M. A.; Cheeseman, J. R.; Montgomery, J. A., Jr.; Vreven, T.; Kudin, K. N.; Burant, J. C.; Millam, J. M.; Iyengar, S. S.; Tomasi, J.; Barone, V.; Mennucci, B.; Cossi, M.; Scalmani, G.; Rega, N.; Petersson, G. A.; Nakatsuji, H.; Hada, M.; Ehara, M.; Toyota, K.; Fukuda, R.; Hasegawa, J.; Ishida, M.; Nakajima, T.; Honda, Y.; Kitao, O.; Nakai, H.; Klene, M.; Li, X.; Knox, J. E.; Hratchian, H. P.; Cross, J. B.; Bakken, V.; Adamo, C.; Jaramillo, J.; Gomperts, R.; Stratmann, R. E.; Yazyev, O.; Austin, A. J.; Cammi, R.; Pomelli, C.; Ochterski, J. W.; Ayala, P. Y.; Morokuma, K.; Voth, G. A.; Salvador, P.; Dannenberg, J. J.; Zakrzewski, V. G.; Dapprich, S.; Daniels, A. D.; Strain, M. C.; Farkas, O.; Malick, D. K.; Rabuck, A. D.; Raghavachari, K.; Foresman, J. B.; Ortiz, J. V.; Cui, Q.; Baboul, A. G.; Clifford, S.; Cioslowski, J.; Stefanov, B. B.; Liu, G.; Liashenko, A.; Piskorz, P.; Komaromi, I.; Martin, R. L.; Fox, D. J.; Keith, T.; Al-Laham, M. A.; Peng, C. Y.; Nanayakkara, A.; Challacombe, M.; Gill, P. M. W.; Johnson, B.; Chen, W.; Wong, M. W.; Gonzalez, C.; Pople, J. A. *Gaussian 03*, revisions B.02 and C.02; Gaussian, Inc.: Wallingford, CT, 2004.

(13) Biegler-König, F.; Schönbohm, J. *J. Comput. Chem.* **2002**, *23*, 1489.

(14) Keith, T. A. *AIMAll97 Package (A3) for Windows*; aim@tkgristmill.com.

CT0501654